Electrical and lattice vibrational behaviors of graphene devices on flexible substrate under small mechanical strain

Yun-Hi Lee and Yoon-Joong Kim

Citation: Applied Physics Letters **101**, 083102 (2012); doi: 10.1063/1.4746285
View online: http://dx.doi.org/10.1063/1.4746285
View Table of Contents: http://scitation.aip.org/content/aip/journal/apl/101/8?ver=pdfcov
Published by the AIP Publishing

Electrical and lattice vibrational behaviors of graphene devices on flexible substrate under small mechanical strain

Yun-Hi Lee[a] and Yoon-Joong Kim[b]
Department of Physics, National Research Laboratory for Nano Device Physics, Korea University, Seoul 136-713, South Korea

(Received 16 April 2012; accepted 1 August 2012; published online 20 August 2012)

We present systematic experimental study on the electrical response and two-phonon Raman scattering mode of graphene under small uniaxial strain. The graphene, which was initially grown by chemical vapor deposition, was transferred to a transparent-flexible-polyethylene-terephthalate substrate. It was found that the electrical resistance increases as the stain is increased after a slight decrease in very small strain regimes of <0.20%. This is due to a relaxation of intrinsic ripples created during the transfer of the graphene to the polyethylene-terephthalate substrate. The gauge factor in the linear response regime was found to be about 22. Also, the 2D Raman bands of the strained graphene showed a distinct red-shift of $-37\,cm^{-1}$ per 1% strain for the $2D^{+}$ mode and $-46\,cm^{-1}$ per 1% strain for the $2D^{-}$ mode. Finally, we determined the Gruneisen parameters of $\gamma_{2\Delta+} \sim 2.05$ and $\gamma_{2\Delta-} \sim 2.55$ for the phonons in free-standing graphene without a substrate. Our results provide electro-mechanical parameters for graphene-based flexible devices and show the potential of graphene for measuring strain in future flexible electronics. © *2012 American Institute of Physics*. [http://dx.doi.org/10.1063/1.4746285]

In crystalline carbon-based materials, the mechanical strain has an influence on the electronic properties.[1–3] Strain arises when the crystal lattice is compressed or stretched out of equilibrium. One interesting observation is that the strain can be used to tune the semiconductor properties of metallic carbon nanotubes (CNTs).[3] As graphene (GL) is also an atomic-thick-elastic material, it is expected to that tuning its electrical properties by mechanical manipulation is possible.[4–7] Unstrained GL at equilibrium is well-known to have two linear energy bands that intersect each other at the *K* and *K* of the first Brillouin zone (BZ). For unstrained GL, the density of states (DOS) vanishes at the Fermi energy E_F (i.e., the Dirac point (E_D)) and thus exhibits typical semi-metallic behavior. By applying strain, the Dirac points should theoretically be driven away from the *K* points with or without opening an energy gap. Sublattice symmetry breaking can give rise to energy gaps in GL on SiO_2, and also, strain with triangular symmetry induces a gauge field with a uniform magnetic field of about 10 T.[8] Therefore, one attractive way to control graphene's electro-magnetic properties is through mechanical strain, which modifies the crystallographic structure of GLs.

Among the various types of strain, uniaxial strain moves the relative positions of the Dirac cones and significantly influences the intervalley double-resonance processes.[4–10] Thus, uniaxial strain, which produces a non-planar-substrate geometry and induces finite perturbations of the Dirac cones, could be utilized to control graphene's properties. Most future applications of GLs are expected in the area of flexible electronics such as wearable devices (i.e., wrist-or-body-mounted-devices). Therefore, bendable-GL/flexible substrate systems are not only simple tools for exploring the physics of graphene materials but also a basis for providing information for realistic applications. In experiment, clarifying the stress-strain relationship is an essential element for exploring new devices such as flexible or electro-mechanical-spinic devices.

The strain dependent characteristics are characterized by the relation between the frequency shift of the Raman band for phonons within the GL, and the applied strain[9–13] or extracting universal Grüneisen parameter,[7,10] which define the thermomechanical properties of a material. Uniaxial strain on graphene has been experimentally applied by bending GL on a plastic substrate such as poly-dimethylsiloxane (PMMA),[9] polyethylene-terephthalate (PET),[7,10] and acryl plate (ACRYL),[13] while using Raman spectroscopy to detect changes of phonons. The most distinct phonon bands in the Raman spectrum of GL-based materials are related to phonons of different points of the first BZ of the GL, i.e., the typical G-band is related to a phonons in the Γ points, whereas the *D*- and 2*D*-bands are due to phonons around the *K* points.[12] Summarizing the results of several recent experimental reports, it was found that the different strain slopes for each Raman signature have been ascribed to factors such as different stress methods, different substrate materials, or different preparation methods. At present, PET is used more widely among the various flexible substrates to fabricate new flexible devices in research and industry. In addition, it is expected that bending, as a tensile type uniaxial stress, is the most common strain applied in real applications.

In this study, we fabricate GL devices using CVD-grown GL, which is more practical for real applications, and study the strain-dependent behaviors of both the electrical and vibrational properties of the GL on a transparent flexible PET substrate. From experimental measurements, we determine the strain sensitivity (% change of resistance per strain) of graphene sheets and suggest some considerations for

[a]Author to whom correspondence should be addressed. Electronic mail: yh-lee@korea.ac.kr.
[b]Present address: Samsung Mobile Display, Asan, Chungnam 336-741, Korea.

future applications. The preparation method was the same as in our previous report[15] on changing from SiO_2/Si substrates to PET. In order to achieve maximum strain, the graphene channel was located at the center of a length of the PET substrate as shown in the Fig. 1. It can be seen that the length of the graphene layers is about 2 times smaller than the substrate length, ensuring a uniform strain on the graphene. The electrical response to strain was measured using two planar Au electrodes (represented by the blue parts in the inverted color images). To check their electrical junction properties, several kinds of gated GL/PET devices were made, and their gate-dependent properties were measured. All tested devices showed semi-metallic properties (not shown in this article) with a positively shifted Dirac voltage of +60 V. In order to study the relationship between the charge transport and structural response (i.e., phonon), Raman measurements for the specimens were performed at room temperature under ambient lighting and humidity. During the measurements, an Ar^+ ion laser with a beam power of 700 $\mu W/\mu m^2$ and a 514 nm wavelength was used to prevent deformation of the atomic GL or damage from laser-induced heating. After the Raman measurements, electrode materials were deposited, and circle arrays of top electrodes were defined on the GL layer.

One can see a typical schematic illustrations of the flexible GL/PET device used in this experiment at the Fig. 1. A bending strain as shown in the Fig. 1 was applied parallel to the length direction of the substrate and was defined by the ratio of substrate thickness to twice the radius of curvature of the flexible GL device. The strain dependence of the electrical current of the GL sheet is presented in Fig. 2(a). The graphene was placed on a 0.3-mm-thick PET substrate. The GL channel was only few sub-nanometers thick, and thus, only the thickness of the PET substrate was considered in the strain calculation. Figure 2(b) shows the electrical two-terminal resistance (R) of the GL/PET under different strains. The electrical resistance obtained from the inverse of the slope of the I-V characteristics increased linearly from 3.69 to 4.19 kΩ when the GL/PET was strained in the range of 0% to 0.77%. The unstrained GL showed a minimum resistance of 3.69 kΩ, and when the strain was removed, the resistance nearly returned to its original magnitude. The linearity of all the I-V characteristics indicates that the ohmic contact properties between the GL and drain/source electrodes remain unchanged whether or not strain is applied. The ohmic characteristics were not disturbed in either the unstrained or strained graphene, hinting at the metallic nature of the GLs.

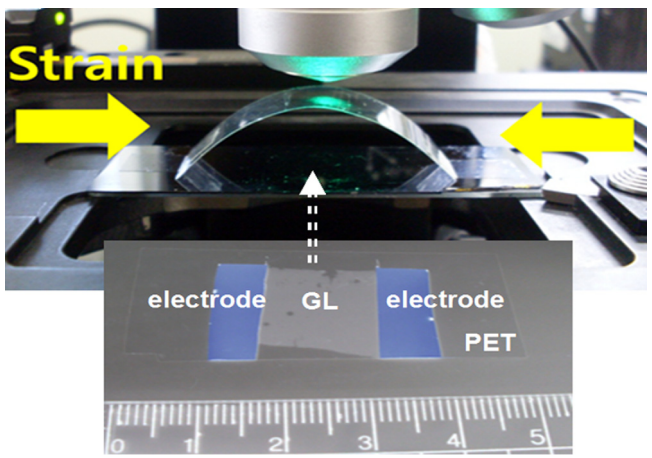

FIG. 1. A schematic illustration of the electrical and Raman measurement for the flexible GL/PET device under strain. Bottom figure shows the real image for the device.

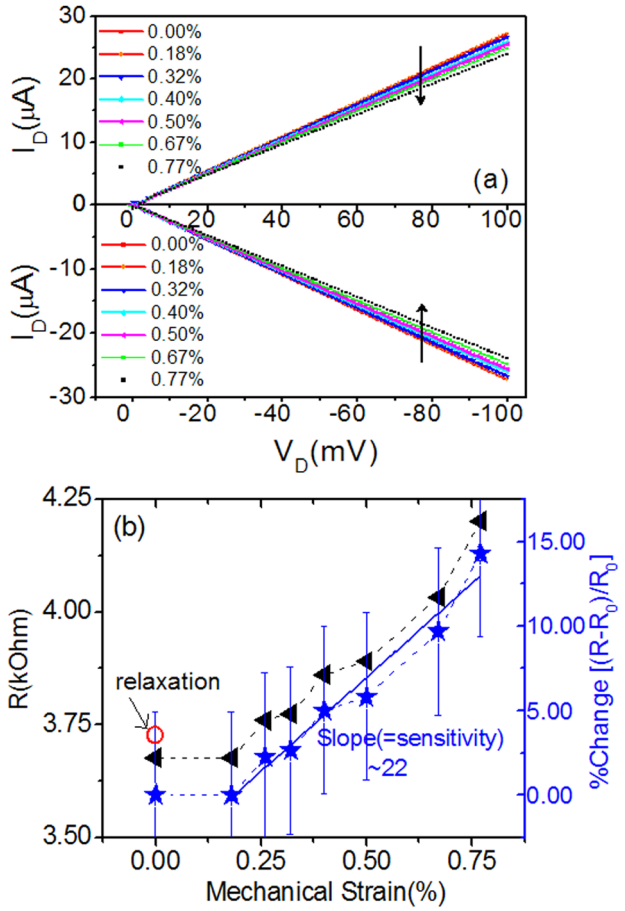

FIG. 2. (a) Current (I) vs drain-source voltage (V) characteristics under strain. (b) Resistance and percent change of the resistance as a function of the applied strain.

The percentage change in the resistance as a function of strain, $(R_{strain} - R_{strain=0}) \times 100/R_{strain=0}$, is shown in the right Y-axis of the Fig. 2(b). The resistivity data in the linear response region were fitted to a linear function. The slope of the linear fit was about 22. Conventionally, the ratio of the relative change in electrical resistance to mechanical strain is defined as the gauge factor (GF), which was ~22 in our case. To examine the repeatability of the results with the same device, we released the strain and confirmed the recovery to nearly the unstrained value, as illustrated by the red circle in Fig. 2(b). The slight deviation of the recovery resistance can be ascribed to the non-flatness of the strained GL via imperfect adhesion to the PET substrate, since the channel length of GL, including ripples, is the same during straining. As it is known that the strain induced by buckling in GL ripples is very small, the change of R due to this intrinsic strain can be thought of as negligible. However, it is noteworthy that the non-flatness of the GL/PEP can cause the scattering of charge carriers, providing a cause for increased R.

Figure 3 shows a typical and a series of Raman spectra of the CVD-grown GL channel/flexible PET. In Figures 3(a)–3(b), the three main modes of GL, the D, G, and 2D

modes, can be observed. The G band, which originates from the in-plane vibrational E_{2g} phonon, is observed at about 1580 cm^{-1}. Unfortunately, because the G band of graphene overlaps with an intense Raman G peak from the PET substrate, clear analysis of the spectrum is hindered. While we cannot discriminate whether the GL or PET is the origin of the G-peak in this data, after subtracting the contribution of the PET substrate, the 2D-mode shows the evolution of a strong GL-only peak as a function of strain. Now, as our interests lie in the characteristics of the Raman band (2D mode) of GL, the mode at about 2680 was decomposed systematically. As expected, the 2D band showed concrete behavior depending on the number of layers of GL. In the case of monolayer GL, a narrow peak of 20-40 cm^{-1} can be seen. Multiple-layer GL has a FWHM of about 50–60 cm^{-1}, which was fitted using multi-peak Lorentzian functions. From the characteristic criterion for the 2D band of GL,[14] the GL channel made in this work was confirmed to be single layer GL though measurements of the beam-exposed area of about $1 \times 1\,\mu m^2$ during the Raman measurements. Figure 3(b) shows the 2D-Raman mode of GL with strains of 0.18%, 0.35%, 0.61%, and 0.78%, and finally, relaxed to the original unstrained state GL. When the strain was increased from 0% to 0.78%, the Raman peak showed a universal red shift of the 2D band over the unstrained graphene. Within the range of small applied strains, the Raman spectra showed meaningful changes as a function of strain. Now, to extract the physical parameters characterizing the response characteristic of the GL to strain, we performed linear fitting to two main 2D Lorentzian components. The fitting results were designated as higher $2D^+$ and lower $2D^-$ frequency. Fig. 3(b) clearly shows the red shift of the two frequencies of the 2D band. It also shows that when the strain is removed, the 2D band shifts upwards and immediately returns to the original peak, indicating good reversibility of the graphene. A blue shift after strain relaxation can clearly be seen, as shown by the blue line in the figure.

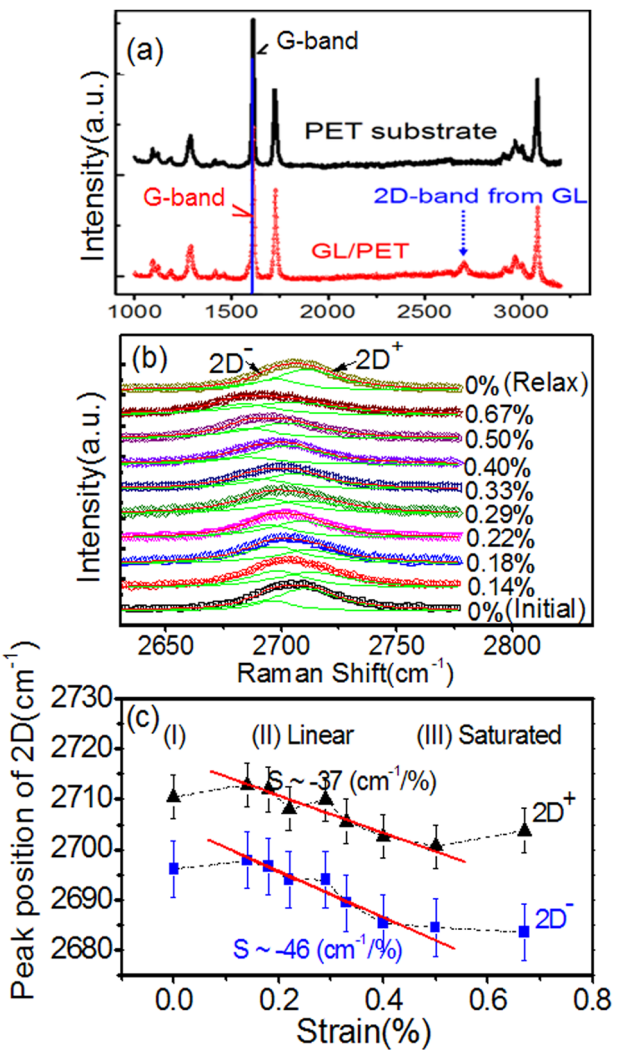

FIG. 3. (a) Raman spectrum for the GL/PET device and the PET substrate. Note: while one cannot discriminate whether the GL or PET is the origin of the G-peak in this data, the 2D band at about 2700 cm^{-1} is only at the GL specimen. (b) Strain dependent 2D-Raman band. The 2D-mode shows the evolution of a strong GL only peak as a function of strain and well fitted to two 2D Lorentzian components, so called $2D^+$ and $2D^-$, respectively. (c) The plots of the shift of the frequency vs the applied strain. In region II, the GL/PET shows linear response and then above a threshold strain the shifts were saturated regardless $2D^+$ or $2D^-$.

The two components exhibit different behaviors corresponding to regions (I), (II), and (III) that correspond to jumping, linear response with strain, and non-linear, even, saturated values (found above a strain of 0.4%), respectively. The initial slope of the higher peak in region (I) is similar to that exhibited by the lower frequency peak, while after the inflection at 0.15% strain, the shift rate of the $2D^+$ frequency with strain is stabilized. In the linear region, region II, the lower frequency component $2D^-$ has a linear dependence on strain with a slope of $-46\,cm^{-1}/\%$, whereas the higher frequency component exhibits a slope of $-37\,cm^{-1}/\%$. When the strain is released, the peak of the 2D-band goes back to almost its original position, indicating good reversibility for the GL on PET substrate. Considering typical spectrometer resolutions of $\sim 1\,cm^{-1}$, it should be noted that the 2D band of GL shows a remarkable sensitivity to strain. Also, we note that no distinct variations in either the peak position of the D-mode or the integrated intensity ratio of the 2D to G peak (I_{2D}/I_G) were observed even after a few stretch-release cycles. This indicates that the straining process does not create new defects in the GL channel.

The plot with standard deviation as errors did not show any discrete jumps under different magnitudes of strain applied in this experiment, which indicates an absence of breaking, cleavage, peeling, or slipping of the GL during the application of the strain. Thus, we can simply understand the fact that the red shift is due to uniform elongation of the C(carbon)-C(carbon) bond length under tensional strain, and this lowers the vibrational frequency of the bonds. The momentum of the emitted phonon by the incident laser beam is determined by the electronic band structure of GL and the phonon dispersion relation around K and K′ points in the reciprocal lattice of the strained GL.[19] In GL without straining, the 2D mode has a single peak, but strained GL has a distorted reciprocal lattice (RL). In this case, one of three K′ points near K in RL moves outward, whereas the other two K′ move the K points inward, resulting in the presence of the two different types of scattering with two different phonons with different momentum. Thus, we could observe splitting of the 2D band. In the following sections, we will analyze the splitting of the two frequencies obtained.

Next, we will find the universal parameters to characterize the strain response. The shift of the frequency is related to uniaxial strain and/or the shear strain on the real lattice of the GL. As the shear strain is known to be negligible, we mainly focused the uniaxial strain and its effect on the phonon modes. For pure A_{1g} symmetry and symmetric strains, the uniaxial-strained Raman frequency is related to stress by the equation[16,17] $\Delta\omega_{strain} = \omega_{strain=0} \cdot \gamma \cdot (\varepsilon_{ll} + \varepsilon_{tt})$, where is the Grüneisen parameter, which describes the effect that the change of volume in a crystal lattice has on the lattice's vibrational properties. ε_{ll} is the uniaxial tensile strain. The resulting strain in the transverse direction ε_{tt} is $-\nu\varepsilon_{\lambda_\lambda}$with a Poisson's ratio of ν. We can use $\nu = 0.3$ for standard PET (Ref. 18) by assuming that an ideal contact is formed between the GL and PET substrate. Combining our experimental slopes for the $2D^+$ and $2D^-$ frequencies as shown in Fig. 3(c), we estimated $\gamma_{2\Delta+} \sim 2.05$ and $\gamma_{2\Delta-} \sim 2.55$. Now, by reinserting these γ values into $\Delta\omega_{strain} = -\omega_{strain=0} \cdot \gamma \cdot \varepsilon_{ll}(1 - 0.33)$, we can estimate the change of frequency/strain, i.e., the strain sensitivity for free-standing GL without the PET substrate. The sensitivity value for the free-standing GL without a PET substrate is estimated to be about $\partial\omega_{2D+}/\partial\varepsilon \sim -37\,\mathrm{cm}^{-1}/\%$ and $\partial\omega_{2D-}/\partial\varepsilon \sim -46\,\mathrm{cm}^{-1}/\%$. These values are smaller than that by Mohiuddin in 2009 of $\partial\omega_{2D}/\partial\varepsilon \sim -83\,\mathrm{cm}^{-1}/\%$ for the mechanical cleaving of GL/PET (720 mm thick, 23 mm long), or the value $\partial\omega_{2D}/\partial\varepsilon \sim -27.8\,\mathrm{cm}^{-1}/\%$ for the mechanical cleaving of GL/PET (unknown thickness) found by Ni *et al.* in 2008. Also, for GL with other substrates, $\partial\omega_{2D+,2D-}/\partial\varepsilon \sim -63.1\,\mathrm{cm}^{-1}/\%, -67.8\,\mathrm{cm}^{-1}/\%$ was found for the mechanical cleaving of GL/ACRYL by Yoon *et al.* in 2011, and $\partial\omega_{2D+,2D-}/\partial\varepsilon \sim -49\,\mathrm{cm}^{-1}/\%, -57\,\mathrm{cm}^{-1}/\%$ was found for the mechanical cleaving of GL/PMMA by Frank *et al.* in 2011. The strain sensitivity in our experiment is smaller than those found in the above experiments. One of the possible causes for the deviation from values found by others for GL/PETs is that the preparation of our GL grown by CVD is different from their mechanical cleaving method. Also, the spontaneous formation of GL ripples while transferring the GL to the PET substrate may induce a lattice mismatch of the elastic modulus between the GL grown at high temperature and the thick PET. Another factor is assumed to be the mixing of zigzag and armchair structures in the GL, because strain was applied in different directions for each structure. The work by Yoon *et al.*[13] reported that the phonon softening rate of Raman 2D modes are orientation-dependent on the incident beam and there are contributions from two kinds of scattering processes[19] such as inner process and outer processes. Also, the theoretical model[18] indicates that the outer process results in the saturated behavior of the frequency shift beyond some critical strain (~3%) for the $2D^+$ and $2D^-$ modes of zigzag GL, whereas armchair GL shows non-saturated behaviors and a linear response within the calculated range of strain. By comparing their experimental results with the model, they concluded that the inner process, i.e., small momentum transfer process, is the dominant cause for the strain-dependent 2D mode of their mechanically cleaving GL specimen. But, in our CVD-grown GL, both the amount of shift of frequency with strain and the saturated behaviors in region III as shown in Fig. 3(c) suggest that the outer process, i.e., large momentum transfer, would be the probable cause for the shift of the frequency and splitting of the 2D-band, and furthermore, the zigzag edge is dominant in our few-centimeter-sized GL.

In summary, the gauge factor in the linear response regime for CVD-grown GL/flexible PET substrate was found to be ~22 under small strain. The 2D Raman bands of the strained graphene showed a distinct red-shift of $-37\,\mathrm{cm}^{-1}$ per 1% strain for the $2D^+$ mode and $-46\,\mathrm{cm}^{-1}$ per 1% strain for the $2D^-$ mode. From the shift of the frequency, we determined the Gruneisen parameters of $\gamma_{2\Delta+} \sim 2.05$ and $\gamma_{2\Delta-} \sim 2.55$ for the phonons in free-standing graphene without a substrate. Also, based on the reported theoretical models for strain-dependent 2D frequency shift, we roughly estimated the edge types of the GL. Our results for the CVD-grown GL can provide electro-mechanical parameters for graphene-based flexible devices and show the potential of graphene for measuring strain within the limited range in future flexible electronics.

This work was supported by the National Research Foundation of Korea (NRF) grant funded by the Korean government (MEST) (No. 2011-0016621) and partially by the National Research Laboratory program (2006-2011).

[1]L. Yang, M. P. Anantram, J. Han, and J. P. Lu, Phys. Rev. B **60**, 13874 (1999).
[2]T. W. Tombler, C. Zhou, L. Alexseyev, J. Kong, H. Dai, L. Liu, C. S. Jayanthi, M. Tang, and S.-Yu. Wu, Nature (London) **405**, 769 (2000).
[3]E. D. Minot, Y. Yaish, V. Sazonova, J.-Y. Park, M. Brink, and P. L. McEuen, Phys. Rev. Lett. **90**, 156401 (2003).
[4]V. M. Pereira and A. H. Castro Neto, Phys. Rev. Lett. **103**, 046801 (2009).
[5]M. A. H. Vozmediano, M. I. Katsnelson, F. Guinea, Phys. Rep. **496**, 109 (2010).
[6]S.-M. Choi, S.-H. Jhi, and Y.-W. Son, Phys. Rev. B **81**, 081407(R) (2010).
[7]Z. H. Ni, Y. Yu, Y. H. Lu, Y. Y. Wang, Y. P. Feng, and Z. X. Shen, ACS Nano **2**, 2301 (2008).
[8]F. Guinea, M. I. Katsnelson, and A. K. Geim, Nat. Phys. **6**, 30 (2010).
[9]O. Frank, G. Tsoukleri, J. Parthenios, K. Papagelis, I. Riaz, R. Jalil, K. S. Novoselov, and C. Galiotis, ACS Nano **4**, 3131 (2010).
[10]T. M. G. Mohiuddin, A. Lombardo, R. R. Nair, A. Bonetti, G. Savini, R. Jalil, N. Bonini, D. M. Basko, C. Galiotis, and N. Marzari, Phys. Rev. B **79**, 205433 (2009).
[11]G. Tsoukleri, J. Parthenios, K. Papagelis, R. Jalil, A. C. Ferrari, A. K. Geim, K. S. Novoselov, and C. Galiotis, Small **5**, 2397 (2009).
[12]E. Corro, M. Taravillo, and V. G. Baonza, Phys. Rev. B **85**, 033407 (2012).
[13]D. Yoon, Y. W. Son, and H. Cheong, Phys. Rev. Lett. **106**, 155502 (2011).
[14]A. C. Ferrari, J. C. Meyer, V. Scardaci, C. Casiraghi, M. Lazzeri, F. Mauri, S. Piscanec, D. Jiang, K. S. Novoselov, S. Roth, and A. K. Geim, Phys. Rev. Lett. **97**, 187401 (2006).
[15]Y.-H. Lee, Y.-J. Kim, and J.-H. Lee, Appl. Phys. Lett. **98**, 133112 (2011).
[16]S. Reich, H. Jantojak, and C. Thomsen, Phys. Rev. B **61**, R13389 (2000).
[17]C. Thomsen, S. Reich, and P. Ordejon, Phys. Rev. B **65**, 073403 (2002).
[18]T. Ma, B. Bhushan, H. Murooka, I. Kobayashi, and T. Osawa, Rev. Sci. Instrum. **73**, 1813 (2002).
[19]E. A. Mafra, S. K. Moujaes, S. K. Doorn, H. Htoon, R. W. Nunes, and M. A. Pimenta, Carbon **49**, 1511 (2011).